CHIN. PHYS. LETT. Vol. 29, No. 8 (2012) 084202

Advanced Aperture Synthesis by Wave-Front Combination in Generalized Phase-Shifting Interferometry *

XU Xian-Feng(徐先锋)[1**], CAI Lü-Zhong(蔡履中)[2], LU Guang-Can(鲁广灿)[1], HAN Guo-Xia(韩国霞)[1], TIAN Yan-Jie(田艳杰)[1], ZHANG Qian(张倩)[1], JIAO Zhi-Yong(焦志勇)[1]

[1]*College of Science, China University of Petroleum (East China), Qingdao 266580*
[2]*Department of Optics, Shandong University, Jinan 250100*

(Received 9 April 2012)

An approach to improve the image quality by aperture synthesis in generalized phase-shifting interferometry is proposed. The aperture of the holographic system is enlarged by increasing the recording area to receive a more diffusive spectrum by moving a singular CCD. The sub-object wave fronts are combined with the index of their intensities. This method can avoid the negative effect of environmental disturbance and improve the synthesis efficiency by hundreds of times. The optical experiments have shown that it is simple and robust to stitch the complex object wave front accurately and to improve the imaging quality greatly, especially for the recording of large scale objects.

PACS: 42.40.Kw, 42.30.Wb, 42.30.Va, 42.30.Rx DOI: 10.1088/0256-307X/29/8/084202

Digital holography has[1−4] been widely applied in various fields of science and engineering since it provides an effective way for wave-front measurement. An off-axis digital holography setup with both the transmission and reflection working modes was demonstrated[5] to achieve the convenience in recording. A portable holographic device working in both in-line transmission and off-axis reflection modes was introduced.[6] This convenient setup and high image quality predicts further brilliant application. To remove the disturbance of a twin image and zero term in in-line holography, phase-shifting interferometry (PSI) technology was introduced by Yamaguchi and Zhang.[7] However, due to some practical factors such as environmental disturbance and limited precision of the phase shifter in recording,phase shift errors exist in the recording process, which in turn induce errors in object wave reconstruction. Corresponding error analysis and correction methods have been proposed to improve the quality of the reconstructed image and most of them are effective in certain circumstances.[8,9] Some phase-shift retrieval algorithms have also been developed to decrease the effects of phase shift errors.[10−12] To achieve the convenience and high precision in PSIs, generalized phase-shifting interferometries (GPSIs) were proposed and the two-step models were studied by Cai *et al.*[13,14] We have also introduced several two-step GPSI methods[15−18] to improve the precision of extracted phase shift and the quality of the reconstructed image.

Another challenging problem is the limited recording size on the CCD chip, which is difficult to improve by current technology. To overcome such obstacles and to enlarge the recording area to collect more information, some researchers[19] have employed two CCDs. However, the lower spatial frequency components between the two CCDs can not be used and it is also difficult to install two cameras on the same plane without knowing the specific locations of their chips. Others have suggested recording multiple sets of sub-frames and then combining them with the correlation method in digital holography or a standard PSI with fixed steps.[20−23] In real practice, however, there are many environmental factors we can not control exactly, and the interference fringe changes more or less at different recording times so that those sub-frames can not form a perfect interference pattern. Mostly those sub-frames are not from the same interference pattern, since the fringe changes at different times. The variations of fringe patterns in sub-frames often make them with small correlation values and therefore incur the failure of aperture synthesis. To solve this problem in PSIs, Li *et al.* recorded 400 frames to find the real frame by iterative calculation of correlation values.[23] This method works effectively, but the computation load is too heavy. Furthermore, all those sub-frame correlation methods mentioned above can not work in GPSIs, because all the phase shift steps between sub-frames generally have different values and most sub-frames are not on the same recording frame.

In this Letter, we present a method using sub-wave-fronts combination instead of sub-hologram combination to realize aperture synthesis with the use

*Supported by the National Natural Science Foundation of China under Grant Nos 60977006, 11004252 and 60777008, and the Natural Science Foundation of Shandong Province under Grant Nos ZR2009GM016 and ZR2010AQ022.

**Corresponding author. Email: xuxf@upc.edu.cn

© 2012 Chinese Physical Society and IOP Publishing Ltd

of only a singular CCD for the purpose of enlarging the recording area and then improving the resolution of the reconstructed image. It can be used not only in PSIs with fixed steps but also GPSIs to improve image resolution and to record large scale objects. Compared with other methods, this method can work with only a few frame numbers needed for GPSIs and then improve the efficiency by hundreds of times. In the following, we will first discuss the corresponding principles and illustrate this method by a flowchart, and then give its optical experiment verification followed by conclusions.

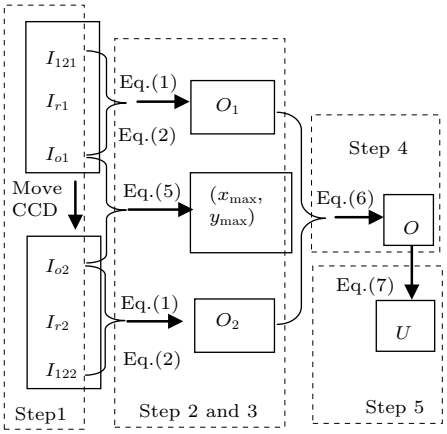


Fig. 1. Flow chart for GPSI aperture synthesis.

It is the object wave on the recording plane that determines the aperture of the imaging system. If we record two or more sets of GPSI sub-frames, retrieve their object wave-fronts respectively, and then combine their object waves, the task of enlarging the recording area can be achieved. The key step here is to combine all the sub-object waves properly. Under most conditions, the size of the CCD chip is very small compared to the recording distance, so the object wave intensities change little if the recording distance varies slightly during the recording process.

For convenience, our method is explained here by taking two sets of GPSI frames as an example. The detailed process for this method is illustrated by Fig. 1. First, we record a set of GPSI frames I_{o1}, I_{r1}, I_{11}, and I_{21}, representing object wave intensity, reference wave intensity, and the intensities of the first and second inteferograms, respectively. Then we move the CCD and record the second set of GPSI inteferograms I_{o2}, I_{r2}, I_{12}, and I_{22}. Third, we can extract the phase shifts as[18]

$$\alpha_p = 2\tan^{-1}\left[\frac{\langle|(I_{1p}-I_{2p})/(4A_{op}A_{rp})|\rangle}{\langle|(I_{1p}+I_{2p}-2A_{op}^2-2A_{rp}^2)/(4A_{op}A_{rp})|\rangle}\right], \quad p=1,2, \tag{1}$$

where the subscript p represents the number of data set recorded consequently. Then the object wave can be expressed as[15]

$$U_p = \frac{I_{1p}-I_{op}-I_{rp}}{2A_{rp}} + i[I_{2p}-I_{1p}\cos\alpha_p-(1-\cos\alpha_p)\cdot(I_{op}+I_{rp})]/(2A_{rp}\sin\alpha_p). \tag{2}$$

Although the two sub-object intensities (with some common area) of I_{o1} and I_{o2} are not recorded at the same time, they can be approximately seen as on the same frame based on the above analysis. Thus the matching location on the recording plane can be found by calculating the correlation function

$$r(x,y) = I_{o1}(x_1,y_1)\otimes I_{o2}(x_2,y_2), \tag{3}$$

where symbol $\otimes$ stands for the correlation of I_{o1} and I_{o2}. The coordinates corresponding to the maximum of r is the right location for the two sub-object waves, denoted as ($x_{\max}$, $y_{\max}$).

We choose two regions on object intensities with $m\times n$ pixels from I_{o1} and I_{o2} respectively, and defined them as i_1 and i_2. Then the correlation value is

$$r = \Big\{\sum i_1 i_2 - \Big(\sum i_1 \sum i_2\Big)/(m\times n)\Big\} \cdot \Big\{\Big[\sum i_1^2 - \Big(\sum i_1\Big)^2/(m\times n)\Big]^{1/2} \cdot \Big[\sum i_2^2 - \Big(\sum i_2\Big)^2/(m\times n)\Big]^{1/2}\Big\}^{-1}. \tag{4}$$

To find the coordinates ($x_{\max}$, $y_{\max}$) corresponding to the maximum r, we must choose different small areas i_2 from I_{o2} to match with i_1 from I_{o1}. If the coordinates of the first pixel in I_{o2} is (x, y), then

$$r(x,y) = i_1(1:m,\,1:n)\otimes i_2[x:(x+m-1),\, y:(y+n-1)], \tag{5}$$

where the colons present the varying ranges of pixels. By iteration of changing coordinates (x,y) we can find ($x_{\max}$,$y_{\max}$), which can be used as the proper mark for the combination of two sub-object wave O_1 and O_2 (with $j\times k$ pixels). Then we have the combined object wave

$$O(M,\,N) = O_1[1:(j-m),\,1:(k-n)] + O_2(x_{\max}:j,\,y_{\max}:k). \tag{6}$$

The new object wave in Eq. (6) has $M\times N$ pixels after combination. Finally, the object wave front can be obtained by the inverse fast Fresnel transform (IFFT) of O of distance z,

$$U(M,\,N) = \mathrm{IFFT}_z\{O(M,N)\}. \tag{7}$$

For clarity, the aperture synthesis method can be summarized briefly as follows:

Step 1. Fix the CCD and record subframes including I_{o1}, I_{r1}, I_{11}, and I_{21}, and then change the location

of the CCD and record the other subframes of I_{o2}, I_{r2}, I_{12}, and I_{22}.

Step 2. Extract two phase shifts α_1 and α_2 by Eq. (1) and two sets of holographic frames respectively. Then retrieve two subwaves O_1 and O_2 further with Eq. (2) separately.

Step 3. Use intensities I_{o1} and I_{o2} as well as Eq. (5) to find the proper coordinates $(x_{\max}, y_{\max})$ by iteration.

Step 4. Combine O_1 and O_2 into a synthesized wave front O by the coordinates $(x_{\max}, y_{\max})$ through Eq. (6).

Step 5. Reconstruct the object wave U on the original plane by Eq. (7).

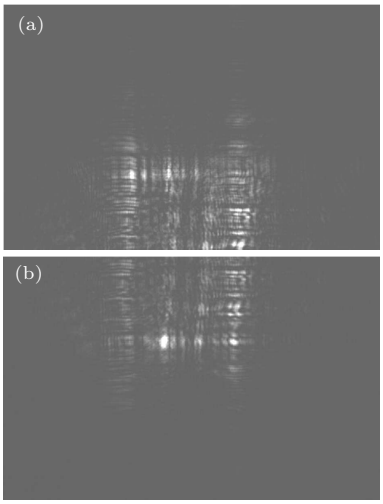


Fig. 2. Two object wave intensities with 1390 pixels: (a) upper part $I_{o1,}$, (b) lower part I_{o2}.

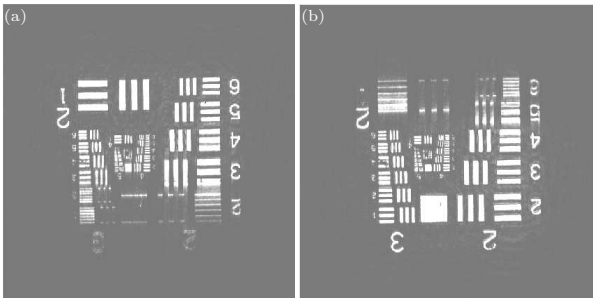


Fig. 3. Two reconstructed images (a) reconstructed from object wave O_1 and (b) reconstructed from object wave O_2.



Fig. 4. The matching model.

Although we have explained the proposed method of aperture synthesis with the example of two-set sub-frames in GPSI, evidently this algorithm can be extended to any sub-frame number by just considering two sets of sub-frames as one and combining the two new ones further. Once all the sub-frames are combined, the original object field can be enlarged by this method.

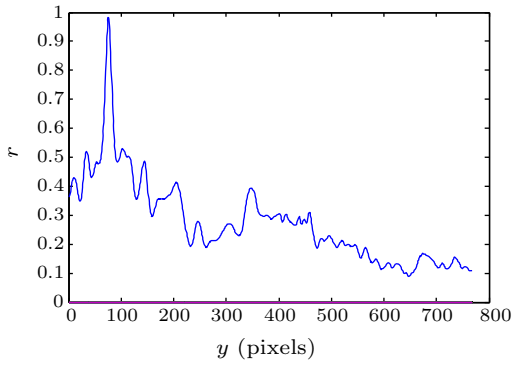


Fig. 5. Correlation value distribution.

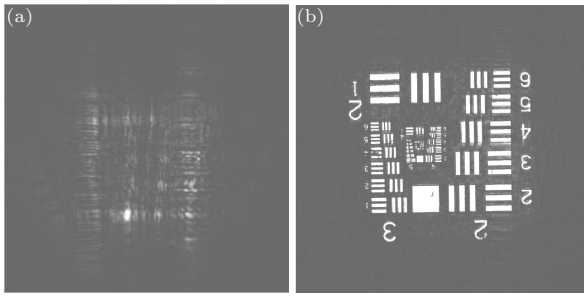


Fig. 6. Reconstructed object intensities after aperture synthesis (a) in the recording plane and (b) in the original plane.

Some optical experiments have been carried out to investigate the performance of our method. The experimental setup is similar to that shown in Fig. 4 of Ref. [17] but with a moveable CCD device. A He–Ne laser with wavelength of 632.8 nm is used as the light source. The central part of 896×1390 pixels of a CCD with pixel size of $6.45\,\mu\text{m} \times 6.45\,\mu\text{m}$ is chosen as the frame size. The distance between the recording plane and the object plane is $z = 26.2\,\text{cm}$. The object is a transparency of USAF resolution target and the reference beam is a normal plane wave. Two sets of GPSI frames are recorded at different CCD locations on the recording plane but with a common folded area. We show the two objective intensities in Figs. 2(a) and 2(b), respectively, which are not located at the center of the two sub-frames for the stitching purpose. We extract α_1 and α_2 by Eq. (1) and two-set frames respectively, and then retrieve two sub-object waves O_1 and O_2 further with Eq. (2). The two object wave-fronts are zero padded into 2350×2350 pixels and then the object waves are reconstructed by Eq. (7) after the IFFT. The object intensity images are amplified, as shown in Figs. 3(a) and 3(b). Evidently, both the lower parts of Fig. 3(a) and the upper part of Fig. 3(b) have low resolution because some higher spatial frequency components are absent. To

find the actual location for two object wave fronts, a small area of 128×1390 pixels is chosen in the intensity I_{o1} (see Fig. 4). We search the $(x_{\max}, y_{\max})$ with Eq. (5) by iteration, and the results are $x_{\max} = 15$ pixels and $y_{\max} = 77$ pixels. To see the effectiveness of this method more obviously, the correlation value distribution in coordinate y is depicted in Fig. 5. It is easy to find that the maximum value is about 0.98 near the ideal value 1. However, the mismatched correlation value decreases very quickly to below 0.5. Therefore, we can determine the actual matching location by this method. With the use of Eq. (6) and coordinates $(x_{\max}, y_{\max})$, the object wavefronts O_1 and O_2 are stitched together into a new O with 1376×1444 pixels. By the zero padding method, the retrieved object waves are enlarged to 2350×2350 pixels on the recording plane, which is amplified, as shown in Fig. 6(a), and then the image is reconstructed on the object plane by Eq. (7) and given in Fig. 6(b) after amplification. Although the intensities of the object wave retrieved by sub-frames have some degradations in the lower and upper parts respectively (see Fig. 3), the combined one has removed those bad effects after aperture synthesis. Many other experiments have led to similar results.

In summary, we have proposed an approach to improve the image quality by aperture synthesis in a two-step GPSI. Firstly, the two sets of sub-interfergrams with marginal folded areas are recorded on the different regions of the recording plane, and then the object waves are reconstructed separately. Secondly, a model is selected from the object wave intensities in the folded area and the stitching location is found by calculating the correlation values between the model and the other sub-objective intensities. Finally, by using the marked coordinates the complex object waves are combined. The optical experiments have shown that our method is robust to improve the quality of the reconstructed image. Although only two sets of GPSI frames are combined here, more sets of interferograms can also be synthesized by this method. For the first time, this method can realize aperture synthesis in the GPSI accurately and can improve calculating efficiency in correlation by almost 400 times. We believe that this technique will find useful applications in future practice, especially when a large scale object is to be recorded.

References

[1] Poon T C, Akin T, Indebetouw G and Kim T 2005 *Opt. Express* **13** 2427
[2] Li J C, Peng Z J and Fu Y C 2011 *Chin. Phys. Lett.* **28** 064201
[3] Ding D H, He Q S, Wang J G, Wu M X and Jin G F 2004 *Chin. Phys. Lett.* **21** 1067
[4] Ma Z H, Wang R K, Zhang F and Yao J Q 2006 *Chin. Phys. Lett.* **23** 366
[5] Ng T W, Peng Z T and Neild A 2010 *Opt. Commun.* **283** 295
[6] Lee M, Yaglidere O and Ozcan A 2012 *Biomed. Opt. Express* **2** 2721
[7] Yamaguchi I and Zhang T 1997 *Opt. Lett.* **22** 1268
[8] Surrel Y 1997 *Appl. Opt.* **36** 271
[9] Patil A, Raphael B and Rastogi P 2004 *Opt. Lett.* **29** 1381
[10] Xu J C, Xu Q and Chai L Q 2008 *Appl. Opt.* **47** 480
[11] Xu J C, Jin W M, Chai L Q and Xu Q 2011 *Opt. Express* **19** 20483
[12] Xu J C, Xu Q, Chai L Q, Li Y and Wang H 2010 *Opt. Express* **18** 20620
[13] Cai L Z, Liu Q and Yang X L 2004 *Opt. Lett.* **29** 183
[14] Cai L Z, Liu Q and Yang X L 2003 *Opt. Lett.* **28** 1808
[15] Xu X F, Cai L Z, Wang Y R, Yang X L, Meng X F, Dong G Y, Shen X X and Zhang H 2007 *Appl. Phys. Lett.* **90** 121124
[16] Xu X F, Cai L Z, Wang Y R, Meng X F, Sun W J, Zhang H, Cheng X C, Dong G Y and Shen X X 2008 *Opt. Lett.* **33** 776
[17] Xu X F, Cai L Z, Wang Y R and Yan R S 2010 *J. Opt.* **12** 015301
[18] Xu X F, Cai L Z, Wang Y R and Li D L 2010 *Chin. Phys. Lett.* **27** 024215
[19] Kreis T and Schlüter K 2007 *Opt. Eng.* **46** 055803
[20] Massig J H 2002 *Opt. Lett.* **27** 2179
[21] Di J L, Zhao J L, Jiang H Z, Zhang P, Fan Q and Sun W W 2008 *Appl. Opt.* **47** 5654
[22] Tippie A E, Kumar A and Fienup J R 2011 *Opt. Express* **19** 12027
[23] Li H Y, Ma Z J, Zhong L Y and L X X 2011 *Acta Opt. Sin.* **31** 0509001